ELSEVIER

Chemical Geology 152 (1998) 211–225

CHEMICAL GEOLOGY
INCLUDING
ISOTOPE GEOSCIENCE

Raman spectra of potassium carbonate and bicarbonate aqueous fluids at elevated temperatures and pressures: comparison with theoretical simulations

John D. Frantz *

Geophysical Laboratory, Carnegie Institution of Washington, Washington, DC 20015, USA

Received 15 October 1997; revised 17 May 1998; accepted 17 May 1998

Abstract

One-molal solutions of potassium carbonate and potassium bicarbonate were investigated by Raman spectroscopy from 22° to 550°C and from 1000 to 2000 bar. Experiments were performed in a special hydrothermal pressure vessel fitted with conical diamond windows. Frequencies and half-widths of the vibrational modes were measured for both carbonate and bicarbonate as a function of temperature and pressure. In the case of potassium carbonate solutions, dissolved bicarbonate appeared with its concentration dramatically increasing with increasing temperature and decreasing density. The opposite behavior occurred in the case of potassium bicarbonate: the relative concentration of dissolved carbonate increased relative to total bicarbonate. In addition, at temperatures above 300°C, dissolved aqueous carbon dioxide appeared with its concentration continuing to increase with increasing temperature and decreasing density. Simulations using theoretically-predicted mass action constants were used to compute changes in solution speciation for these solutions as they were subjected to increased temperature and pressure. Results resulting from these predictions matched those discovered in the spectral measurements. © 1998 Elsevier Science B.V. All rights reserved.

Keywords: Potassium carbonate; Potassium bicarbonate; Raman spectroscopy

1. Introduction

The composition of natural high-temperature, high-pressure fluids in the Earth's crust have a significant influence on the evolution and resulting mineral paragenesis of igneous and metamorphic rock suites. Of particular interest are fluids containing C–O–H gas mixtures due to the frequent occurrence of carbon dioxide and methane in hydrothermal fluids and the common presence of carbon-bearing minerals in associated rock suites. These fluids, mixtures of gases, dissolved electrolytes and water, exist either as a single supercritical phase or as a mixture of two immiscible phases (Zhang and Frantz, 1989, 1992). Though considerable effort has been devoted towards understanding gas equilibria in this system (Eugster and Skippen, 1967; Greenwood, 1969, 1973; Kerrick and Jacobs, 1981; Holloway,

* Fax: +1 202 686 2419; e-mail: frantz@gl.ciw.edu

0009-2541/98/$ - see front matter © 1998 Elsevier Science B.V. All rights reserved.
PII: S0009-2541(98)00058-8

Table 1
Solution compositions of one-molal potassium carbonate and one-molal potassium bicarbonate at 25°C, 1 atm

Species	K_2CO_3	$KHCO_3$
$KOH^{\cdot}$	1.47×10^{-3}	1.67×10^{-7}
K^+	1.49×10^{0}	9.27×10^{-1}
OH^-	5.37×10^{-3}	1.04×10^{-6}
H^+	3.74×10^{-12}	2.05×10^{-8}
HCO_3^-	6.08×10^{-3}	8.96×10^{-1}
CO_3^{2-}	5.36×10^{-1}	1.19×10^{-2}
CO_2 (aq)	2.50×10^{-8}	1.92×10^{-2}
KCO_3^-	4.06×10^{-1}	6.80×10^{-3}
$K_2CO_3^{\cdot}$	5.10×10^{-2}	4.96×10^{-4}
$KHCO_3^{\cdot}$	7.62×10^{-4}	6.54×10^{-2}

1984; Saxena and Fei, 1988), little attention has been devoted towards the investigation of the relative concentrations of dissolved carbon-bearing electrolytes. The complexity of experimentally investigating such fluids is due to: (1) their dependence on oxidation fugacity; (2) the number of mass action constants needed to describe the system; and (3) the low solubilities of many of the salts. To address these difficulties, a combined experimental and theoretical approach has been adopted using in-situ spectroscopic measurements in combination with predictive thermochemical calculations on relatively soluble solutions in the potassium carbonate–water system. Such solutions are amenable to Raman studies and can serve to test the theoretically-predicted mass-action constants used to describe the distribution of dissolved species in carbonate-bearing fluids.

Davis and Oliver (1972) in their study of potassium carbonate solutions described the Raman spectra of aqueous carbon dioxide, bicarbonate and carbonate ions at room temperature and pressure. They demonstrated the presence of a limited amount of interaction between molecular carbon dioxide and water with only minor amounts of CO_2 existing as H_2CO_3. They deciphered the vibrational symmetries

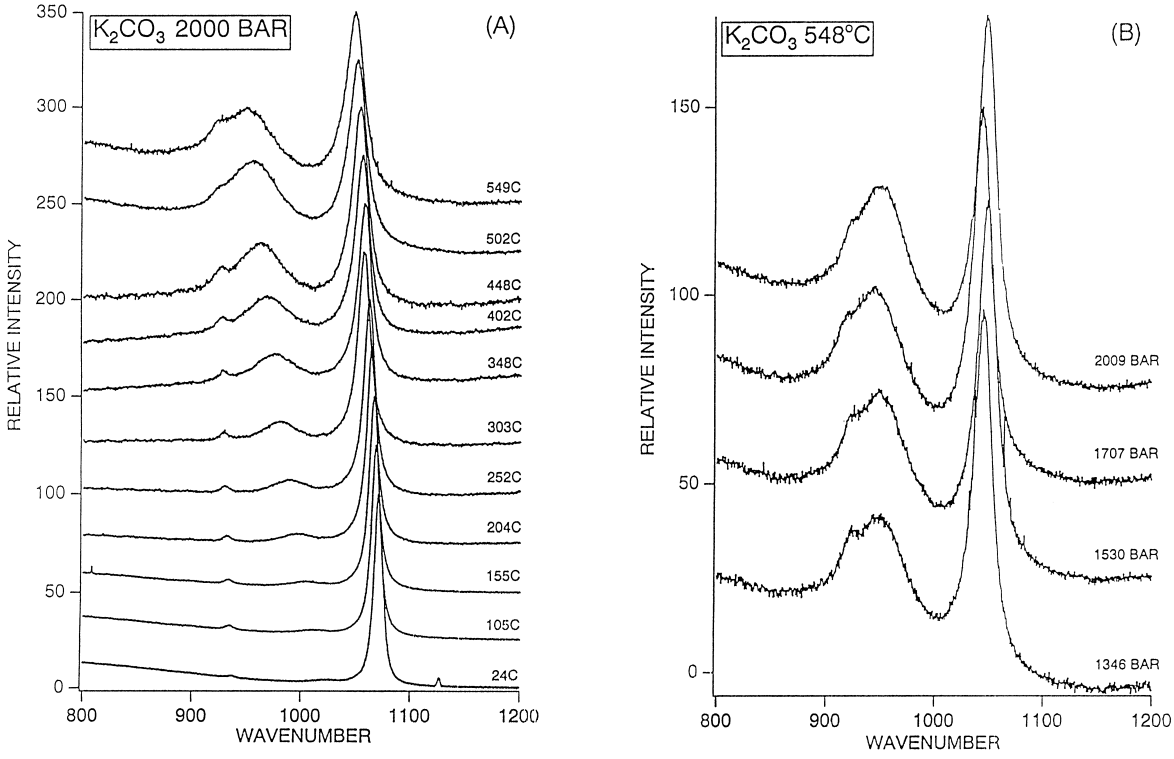

Fig. 1. Raman spectra of aqueous one-molal potassium carbonate solutions. (A) Spectra collected at varying temperatures at 2000 bar. (B) Spectra collected at 548°C at varying pressures.

of the bicarbonate and carbonate ions, suggested that small amounts of carbonate coexist with bicarbonate in potassium bicarbonate solutions and demonstrated the dependence of the ratio of dissolved carbonate to bicarbonate on pH. Oliver and Davis (1973) investigated the vibrational spectra of bicarbonate and carbonate solutions containing lithium, sodium, potassium, rubidium, and cesium at room temperature and pressure. They demonstrated that carbonate and bicarbonate spectra at 25°C, 1 atm are independent of concentration and the alkali metal and thus saw no evidence of ion-pairing. Kruse and Franck (1982) investigated two molar potassium bicarbonate solutions to 300°C suggesting that increased abundances of carbonate might be forming at the expense of bicarbonate with increasing temperature. They also determined the presence of bicarbonate ions in 3% CO_2–H_2O mixtures at 34°C, 750 bar. Dubessy et al. (1997) investigated the behavior of carbon dioxide–water mixtures using synthetic fluid inclusions. Evidence of molecular interactions between carbon dioxide and water were documented under hydrothermal conditions.

2. Experimental methods

The Raman spectra of potassium carbonate- and bicarbonate-bearing aqueous solutions were collected

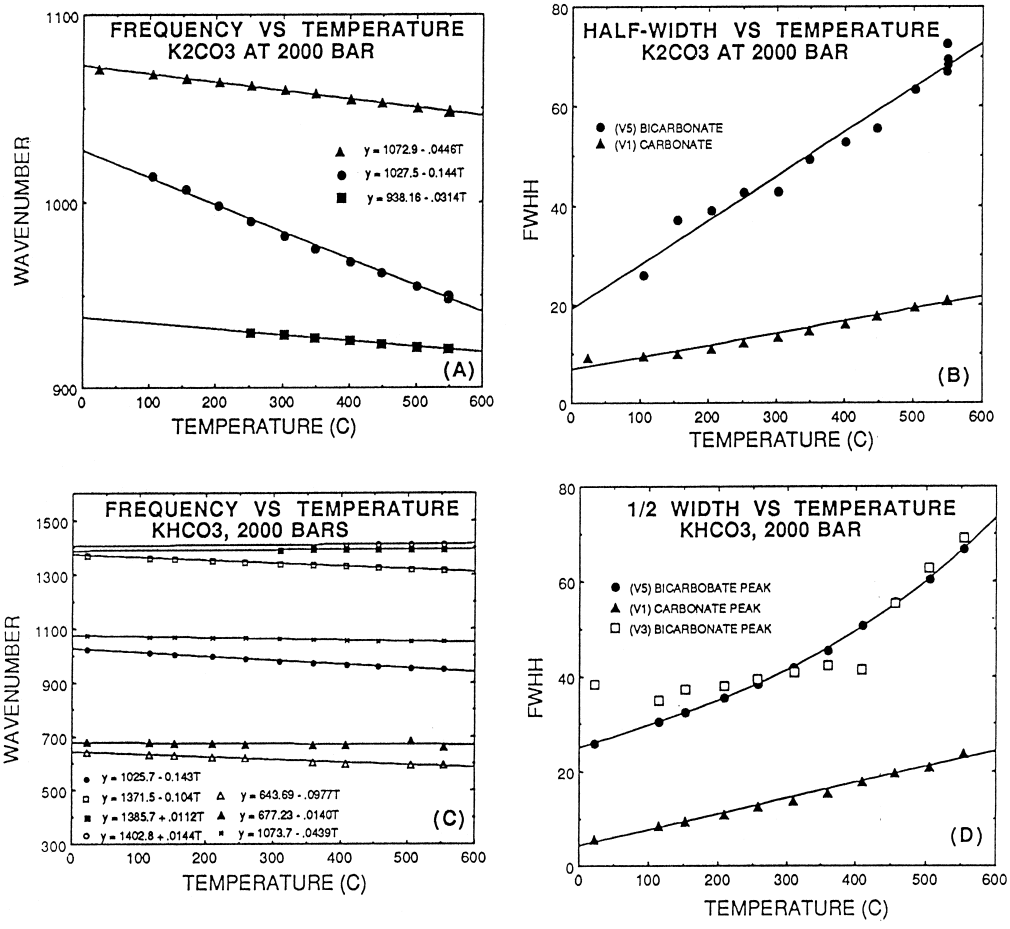

Fig. 2. Peak frequencies and half-widths as a function of temperature at 2000 bar for one-molal potassium carbonate and potassium bicarbonate solutions.

using a specially-designed hydrothermal pressure vessel with diamond windows (Frantz, 1981; Frantz et al., 1993). The disk-shaped pressure vessel (diameter: 2 in.; height: 1 in.) contains two conical low-fluorescence diamond windows set at right angles to one another. The cell, containing a $Pt–Pt_{90}Rh_{10}$ thermocouple extending into the fluid cavity, is heated using two spirally-wound platinum resistance furnace elements. The fluid is introduced and pressure is generated using a small stainless-steel intensifier. Pressure is measured using an Autoclave® 0–60 000 psi transducer. Pressure calibration of the transducer was accomplished using a recently calibrated Heise® bourdin-tube gauge. A melting point furnace was used in the temperature calibration of the thermocouples. Temperature errors are thought to be ± 5°C; pressure errors, ± 10 bar. The pressure vessel and much of the pressure-generating apparatus are gold plated to reduce the effects of corrosion and therefore inhibit fluorescence. Prior to use, the cell and associated pressure-generating apparatus were repeatedly cleaned with ultra-pure hexane, methanol, and triple-distilled water. Great care was taken in filling the system with the sample fluid in order to prevent the introduction of dust and bubbles.

The optical cell was used in conjunction with a Dilor® XY confocal Raman spectrometer equipped with an intensified diode array detector. Gratings with 1800 lines/mm yield a spectral resolution of approximately 1 cm^{-1}. The 514.5 nm line of a SpectroPhysics® model 2025 Ar^{+} laser operating at 1.8 W was used for sample excitation. The spectrometer was calibrated with respect to wavenumber using both the frequency of the laser line and a mercury lamp. Collection of the scattered light was at 90°C to the incident radiation. Experiments were performed by first incrementing temperature and measuring spectra at varying pressures. Signal collection times averaged 300 seconds. Analyses of the resulting Raman spectra were accomplished using computer algorithms contained in the software package Igor Pro (WaveMetrics®).

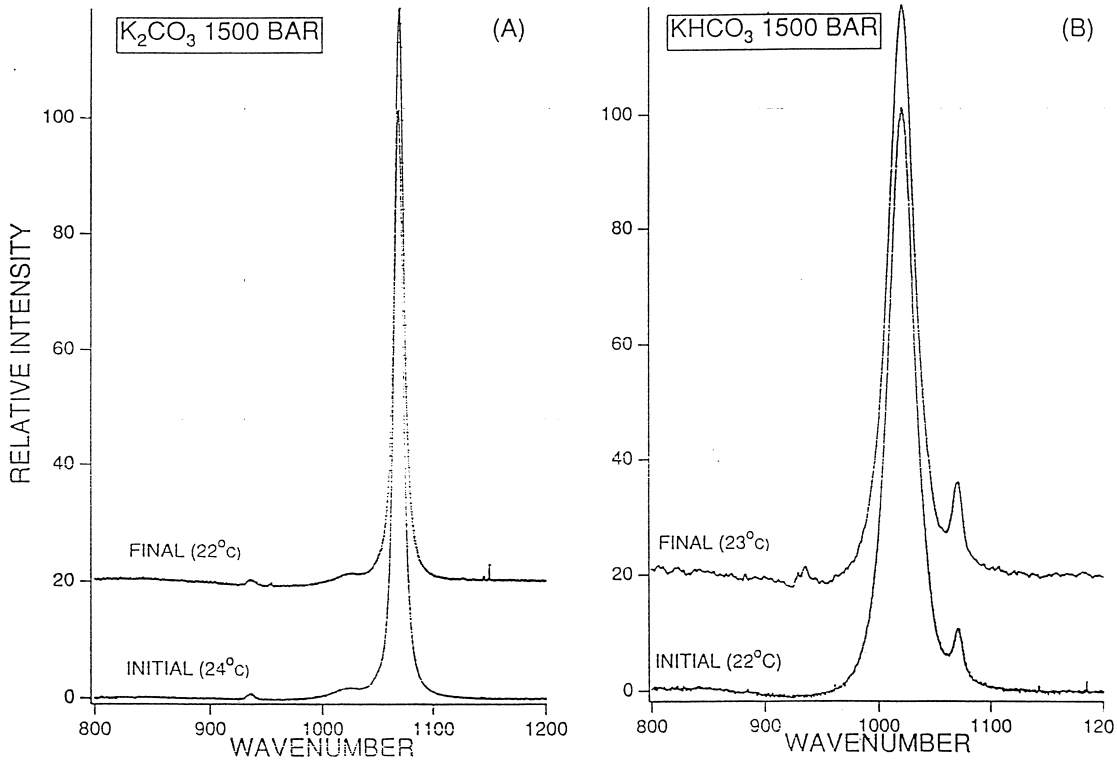

Fig. 3. Comparison of Raman spectra taken at standard temperature at 1500 bar before and after high temperature measurements. (A) Potassium carbonate; (B) Potassium bicarbonate.

The one-molal potassium carbonate aqueous solution was prepared from granular anhydrous potassium carbonate reagent (Alfa®, Lot No. 010686) and doubly-distilled water; the one-molal potassium bicarbonate solution, from granular potassium hydrogen carbonate (Aldrich®, Lot No. 06930AQ). The concentration of both solutions were verified after preparation by analysis of potassium using atomic absorption spectrometry. No effort was made to degas or equilibrate the solution with atmospheric carbon dioxide.

3. Experimental results

Potassium carbonate in binary K_2CO_3–H_2O aqueous solutions exists primarily as potassium and carbonate ions under standard temperature and pressure conditions (Table 1). Values of pH are calculated to be in the range of 11.4 though they were not measured. There is, however, a small abundance of bicarbonate ions. The isolated carbonate ion (D_{3h} symmetry) exhibits four fundamental modes of vibration (Davis and Oliver, 1972). Of these, only

Table 2
Spectral parameters. One-molal potassium carbonate solution

T (°C)	Pressure (bar)	Carbonate (ν_1)			Bicarbonate (ν_5)			920 Peak	Mole fraction	
		Frequency	Area	FWHH	Frequency	Area	FWHH	Frequency	HCO_3	CO_3
24	2009	1071.0	1321	9.1	NA	NA	NA	NA	NA	NA
24	1522	1070.8	1330	9.0	NA	NA	NA	NA	NA	NA
24	1019	1070.5	1348	8.9	NA	NA	NA	NA	NA	NA
105	2004	1068.4	1324	9.6	1011.9	NA	15.3	NA	0.011	0.989
105	1539	1068.1	1286	9.7	1010.5	NA	24.5	NA	0.026	0.974
105	1039	1067.8	1286	9.7	1008.7	NA	10.9	NA	0.007	0.993
155	2015	1066.5	1295	10.2	1003.6	NA	18.0	NA	0.022	0.978
155	1490	1066.1	1205	10.4	1002.4	NA	12.8	NA	0.015	0.985
154	1061	1065.8	1121	10.6	1000.5	NA	17.1	NA	0.020	0.980
204	2008	1064.4	1172	11.2	996.2	NA	19.3	NA	0.040	0.960
201	1511	1064.0	1035	11.2	995.3	NA	18.8	NA	0.042	0.958
203	1059	1063.7	864	11.4	994.2	NA	18.2	NA	0.046	0.954
252	2020	1062.1	1068	12.3	990.0	265	42.7	930.1	0.199	0.801
252	1528	1061.7	922	12.2	988.4	185	36.2	930.1	0.167	0.833
253	1036	1061.3	792	12.5	987.3	154	34.8	929.3	0.162	0.838
303	2018	1059.9	919	13.5	982.0	333	42.8	928.6	0.266	0.734
301	1529	1059.5	835	13.5	981.4	235	37.8	928.4	0.220	0.780
301	1064	1059.0	759	13.6	980.1	194	35.4	928.0	0.203	0.797
348	1996	1057.7	866	14.8	974.9	472	49.2	927.4	0.353	0.647
350	1512	1057.3	821	14.9	974.0	346	42.5	927.6	0.296	0.704
351	1018	1056.8	775	15.0	972.5	355	45.1	927.3	0.315	0.685
402	2016	1055.2	912	16.2	968.0	681	52.8	925.7	0.427	0.573
399	1522	1054.8	912	16.2	966.7	585	49.2	926.3	0.391	0.609
399	1045	1054.3	936	16.3	965.5	647	52.8	925.7	0.409	0.591
448	2043	1053.1	877	17.7	962.0	839	55.6	924.0	0.489	0.511
448	1545	1052.6	1015	18.0	961.3	859	54.7	924.5	0.458	0.542
448	1052	1052.1	1065	17.8	959.6	765	52.1	924.5	0.418	0.582
502	2019	1050.4	1737	19.4	955.3	2231	63.3	922.1	0.562	0.438
508	1527	1049.6	1761	19.1	953.1	2230	66.2	921.0	0.559	0.441
508	1041	1049.0	1677	19.2	949.2	1826	66.7	942.3	0.521	0.479
549	2009	1048.7	1690	20.8	950.3	2516	68.4	920.9	0.598	0.402
548	1709	1048.3	1662	20.7	950.1	2214	66.9	921.2	0.571	0.429
549	1530	1048.1	1610	20.7	948.8	2114	69.4	920.7	0.568	0.432
548	1346	1047.7	1568	20.7	948.2	1981	72.5	920.8	0.558	0.442

NA = not analyzed.
FWHH = full width at half height.

three are Raman active. The principal mode, the symmetric stretch $\nu_1(A'_1)$ occurs at 1064 cm^{-1}. The modes $\nu_3(E')$ and $\nu_4(E')$ occur at 1436 (1380) cm^{-1} and 684 cm^{-1}, respectively. Interaction between potassium and carbonate if associated as ion pairs at standard temperature and pressure would not be Raman active due to the ionic nature of their bond.

Binary solutions of $KHCO_3$–H_2O, on the other hand, contain primarily potassium and bicarbonate ions at standard temperature and pressure (Table 1). Values of pH are in the range of 7.7; potassium bicarbonate solutions appear to contain minor amounts of carbonate ions. Assuming the $C_s(\sigma_h)$ symmetry model (Davis and Oliver, 1972), nine fundamental modes of vibration exist for the bicarbonate ion. Of these an intense C–OH stretching mode ($\nu_5(A')$) is present at 1017 cm^{-1}. Bands representing the (OH)CO bending mode ($\nu_7(A')$) and the CO_2 bending mode ($\nu_6(A')$) are at 632 and 672 cm^{-1}, respectively. The COH bending mode ($\nu_4(A')$) is at 1302 cm^{-1} and the symmetric CO stretch ($\nu_3(A')$) is at 1360 cm^{-1}.

Potassium carbonate and potassium bicarbonate solutions at standard temperatures and pressures (Table 1) contain only minor molal amounts of aqueous carbon dioxide (2.5×10^{-8} and 1.9×10^{-2}, respectively). Molecular carbon dioxide, $D_{\infty h}$ symmetry, exhibits three fundamental vibrational modes: a symmetric stretching mode (ν_1); a doubly degenerate bending mode (ν_2); and an antisymmetric stretching mode (ν_3). Of these, only the symmetric stretching mode is Raman active. Carbon dioxide does, however, exhibit Fermi resonance due to the interaction of the Raman-active overtone of the bending mode (ν_2) with the fundamental stretching mode (ν_1) resulting in the fermi diad with peaks at 1388 and 1285 cm^{-1} (Colthup et al., 1975). In addition to the fermi diad, carbon dioxide at elevated temperatures

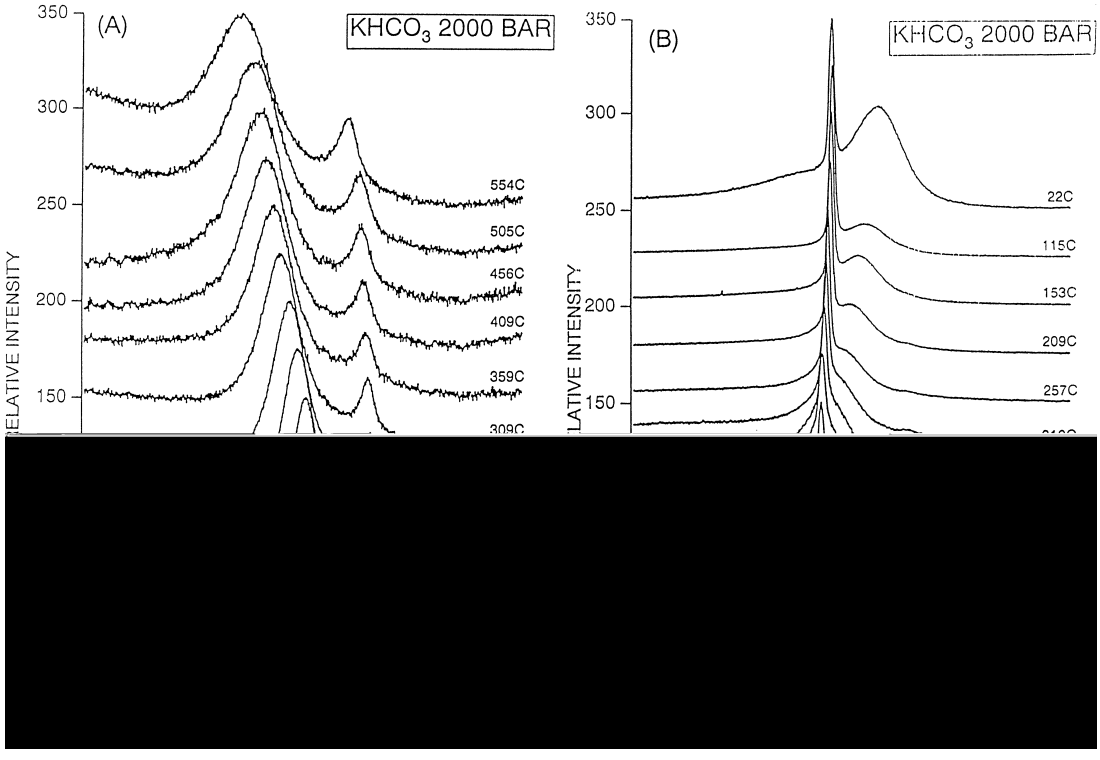

Fig. 4. Raman spectra of aqueous one-molal potassium bicarbonate solutions. (A) Spectra collected in the spectral range 800 to 1200 cm^{-1} at varying temperatures at 2000 bar. (B) Spectra collected in the spectral range 1200 to 1500 cm^{-1} at varying temperatures at 2000 bar.

considering the following relationship between species concentration and the intensity of its Raman peak:

$$I_i = \gamma_i C_i \quad (8)$$

where I_i is the intensity of the peak representing the ith species; C_i is the concentration of species i in molarity; and γ_i is the scattering coefficient of the ith species. Considering the ratio of the intensities of two species, Eq. (8) becomes:

$$I_1/I_2 = (\gamma_1/\gamma_2)(C_1/C_2) \quad (9)$$

Assuming: (1) peak area ratios are proportional to peak intensities; (2) the scattering efficiency of all carbonate species are equal; and (3) the scattering efficiency of all bicarbonate species are equal,

$$A_{\text{carb}}/A_{\text{bicarb}} = \Gamma(m_{\text{carb}}/m_{\text{bicarb}}) \quad (10)$$

where A_{carb} is the area under the peak representing total carbonate; A_{bicarb} is the area under the peak representing total bicarbonate; Γ is the ratio of the scattering coefficients; and m_{carb} and m_{bicarb} represent the molal concentrations of total carbonate and bicarbonate, respectively. Using the data for the total carbonate and bicarbonate peak areas in Tables 2 and 3 for the K_2CO_3 and $KHCO_3$ solutions in conjunction with the total computed concentrations representing the various carbonate and bicarbonate species (shown in Fig. 8(C) and Fig. 9(C), respectively), values of the ratio of the scattering coefficients Γ have been be computed for each of the two solutions. If the previously-stated assumptions and the theoretical simulations of species distributions are correct, the scattering coefficient ratios for both solutions should be identical at fixed temperature and pressure. As seen in Fig. 10 for solutions at 2000 bar, they are surprisingly close considering the inherent errors in the computations. The ratio of the scattering coefficient of carbonate to bicarbonate is seen to decrease with increasing temperature which may not be surprising considering the large differences in the temperature dependence of both their frequencies and half-widths with increasing temperature. The pressure dependence of this ratio is undetectable in the calculations.

The calculations of scattering coefficient ratios lends credence to the theoretical calculations of species distributions at elevated temperatures and pressures. Not only do the temperature-dependent trends demonstrated by comparison of Fig. 7(A),(B) with Fig. 8(C)Fig. 9(C) agree, but the actual ratios of concentrations of the computed species distributions agree with observed Raman measurements (as demonstrated in Fig. 10). The apparent differences between these two sets of figure are reconciled by the cross-sectional differences of the Raman scattering. The results thus indirectly verify the presence of the potassium carbonate and bicarbonate ion pairs.

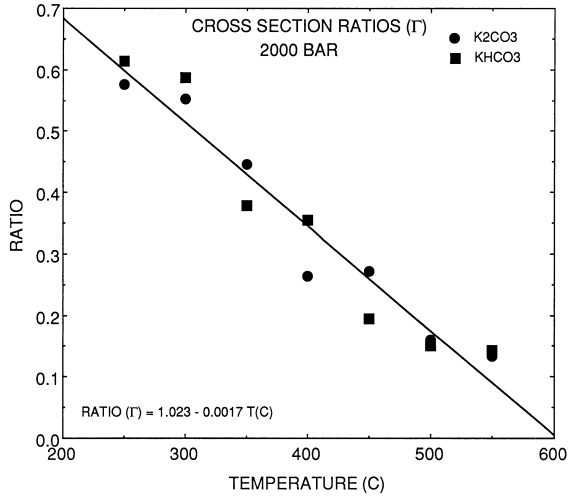

Fig. 10. Variation of the Raman scattering coefficient ratio (Γ) of total carbonate as a function of temperature at 2000 bar. The filled circles represent ratios calculated for one-molal potassium carbonate solutions; the filled squares, for one-molal potassium bicarbonate solutions. The line represents a least-squares fit to all the data.

5. Conclusions

The behavior of complicated systems under hydrothermal conditions such potassium carbonate solutions are poorly known due to the lack of experimentally-derived data. Characterization requires the *simultaneous* determination of numerous mass action constants. Current efforts are focusing on theoretical estimates of the thermodynamic properties of dissolved species of complicated systems such as this (i.e., Sverjensky et al., 1997). The experimental bases for many of the predictions, however, are frequently lacking. In the case of hydrothermal fluids containing potassium carbonate and potassium bicarbonate,

spectroscopic investigations of the presence and relative intensities of peaks representing total dissolved carbonate, bicarbonate, and aqueous carbon dioxide support the trends which can be predicted by theoretical simulations. The interplay between theoretical prediction of speciation in complicated hydrothermal fluids and the monitoring of the presence and relative abundance of dissolved species in experimental fluids using spectroscopic measurements should be a constructive avenue in furthering our knowledge of supercritical fluids.

Acknowledgements

The author is indebted to B.O. Mysen, D.A. Sverjensky, R. Arvidson, E. Oelkers, S. Lvon, and F.T. Mackenzie for their assistance. The project was supported by the Carnegie Institution of Washington and a grant from the Centre National de la Recherche Scientifique through its Programme International de Cooperation Scientifiique (PICS #142).

References

Colthup, N.B., Daly, L.H., Wiberley, S.E., 1975. Introduction to Infrared and Raman Spectroscopy. Academic Press, New York, 523 pp.

Davis, A.R., Oliver, B.G., 1972. A vibrational-spectroscopic study of the species present in the CO_2–H_2O system. J. Solution Chem. 1 (4), 329–338.

Dubessy, J., Moissette, A., Bakker, R., Frantz, J.D., Zhang, Y.-G., 1997. High temperature Raman spectroscopic study of H_2O–CO_2–CH_4 mixtures in synthetic fluid inclusions: first insights on molecular interactions and analytical implications. Eur. J. Mineral., in review.

Eugster, H.P., Skippen, G.B., 1967. Igneous and metamorphic reactions involving gas equilibria. In: Abelson, P.H. (Ed.), Researches in Geochemistry. Wiley, New York, pp. 492–520.

Frantz, J.D., 1981. High-pressure, high-temperature optical cell for Raman spectroscopy. Carnegie Institution of Washington Yearbook 80, 406–408.

Frantz, J.D., Marshall, W.L., 1982. Electrical conductance and ionization constants for calcium chloride and magnesium chloride in aqueous solutions at temperatures to 600°C and pressures to 4000 bar. Am. J. Sci. 282, 1666–1693.

Frantz, J.D., Popp, R.K., Boctor, N.Z., 1981. Mineral-solution equilibria: V. Solubilities of rock-forming minerals in supercritical fluids. Geochim. Cosmochim. Acta 45 (1), 69–77.

Frantz, J.D., Dubessy, J., Mysen, B.O., 1993. An optical cell for Raman spectroscopic studies in supercritical fluids and its application to the study of water to 500°C and 2000 bar. Chem. Geol. 106, 9–26.

Frantz, J.D., Dubessy, J., Mysen, B.O., 1994. Ion-pairing in aqueous $MgSO_4$ solutions along an isochor to 500°C and 11 kbar using Raman spectroscopy in conjunction with the diamond-anvil cell. Chem. Geol. 116, 181–188.

Greenwood, H.J., 1969. The compressibility of gaseous mixtures of carbon dioxide and water between 0 and 500 bar pressure and 450° and 800°C. Am. J. Sci. A 267, 191–208.

Greenwood, H.J., 1973. Thermodynamic properties of gaseous mixtures of H_2O and CO_2 between 450° and 800°C and 0 to 500 bar. Am. J. Sci. 273, 191–208.

Helgeson, H.C., 1969. Thermodynamics of hydrothermal systems at elevated temperatures and pressures. Am. J. Sci. 267, 729–804.

Holloway, J.R., 1984. Graphite–CH_4–H_2O–CO_2 equilibria at low-grade metamorphic conditions. Geology 12, 455–458.

Johnson, J.W., Oelkers, E.H., Helgeson, H.C., 1992. SUPCRT92: a software package for calculating the standard molal thermodynamic properties of minerals, gases, aqueous species, and reactions from 1 to 5000 bar and 0 to 1000°C. Computers and Geosciences 18 (7), 899–947.

Kerrick, D.M., Jacobs, G.K., 1981. A modified Redlich–Kwong equation for H_2O, CO_2 and H_2O–CO_2 mixtures at elevated pressures and temperatures. Am. J. Sci. 281, 735–767.

Kruse, R., Franck, E.U., 1982. Raman spectra of hydrothermal solutions of CO_2 and HCO_3 at high temperatures and pressures. Ber. Bunsenges Phys. Chem. 86, 1036–1038.

Oliver, B.G., Davis, A.R., 1973. Vibrational spectroscopic studies of aqueous alkali metal bicarbonate and carbonate solutions. Can. J. Chem. 51, 698–702.

Saxena, S.K., Fei, Y., 1988. Fluid mixtures in the C–H–O system at high pressure and temperature. Geochim. Cosmochim. Acta 52, 505–512.

Sverjensky, D.A., Shock, E.L., Helgeson, H.C., 1997. Prediction of the thermodynamic properties of aqueous metal complexes to 1000°C and 5 kb. Geochim. Cosmochim. Acta 61 (7), 1359–1412.

Zhang, Y.-G., Frantz, J.D., 1989. Experimental determination of the compositional limits of immiscibility in the system $CaCl_2$–H_2O–CO_2 at high temperatures and pressures using synthetic fluid inclusions. Chem. Geol. 74, 289–308.

Zhang, Y.-G., Frantz, J.D., 1992. Hydrothermal reactions involving equilibrium between minerals and mixed volatiles: 2. Investigations of fluid properties in the CO_2–CH_4–H_2O system using synthetic fluid inclusions. Chem. Geol. 100, 51–72.